Journal of Alloys and Compounds 618 (2015) 217–221

Contents lists available at ScienceDirect

Journal of Alloys and Compounds

journal homepage: www.elsevier.com/locate/jalcom

Improved characteristics for chemically grown Cu_2SnS_3 promising solar absorbers through the use of TritonX-100® surfactant

S. Yaşar [a,*], S. Kahraman [a,b], S. Çetinkaya [a], İ. Bilican [c]

[a] Semiconductor Research Laboratory/Group, Physics Department, Mustafa Kemal University, Hatay, Turkey
[b] Department of Metallurgy and Material Engineering, Faculty of Technology, Mustafa Kemal University, Hatay, Turkey
[c] Scientific and Technological Applications and Research Center, Aksaray University, Aksaray, Turkey

ARTICLE INFO

Article history:
Received 3 July 2014
Received in revised form 16 August 2014
Accepted 23 August 2014
Available online 3 September 2014

Keywords:
Cu_2SnS_3
Sol–gel spin coating
Thin film
Solar cell
Surfactant

ABSTRACT

In this paper, we report, for the first time, the results of the TritonX-100® surfactant assisted growth of Cu_2SnS_3 thin films obtained by using sol–gel spin coating method and a subsequent annealing in a sulfur atmosphere. Structural, morphological, compositional, photo-electrical investigations have been carried out. X-ray diffraction patterns of the samples matched well with the reference Cu_2SnS_3 pattern and indicated the polycrystalline nature of the films. Crystallite size of the films increased whereas surface roughness of the films decreased with increasing Triton-X100® content. The surface of the samples has been smoother with Triton-X100® inclusion. The photo-sensitivity of the n-Si/CTS structures has been confirmed through photo-transient current measurements. An increment was observed in the photo-induced current values of the samples with increasing Triton-X100® content and was attributed to transport of photo-induced electrons facilitated with decreasing recombination resulted from the surface enhancement of the films. Electrical conduction mechanism of the films was investigated with resistance–temperature measurements. It has been revealed that TritonX-100® surfactant assisted growth is a promising way to improve conversion efficiency of Cu_2SnS_3 based solar cells.

© 2014 Elsevier B.V. All rights reserved.

1. Introduction

Cu–Sn–S compounds are promising solar absorber materials for the production of cheaper large-scale thin film solar cells due to the abundancy of the constituents in the earth's crust [1–6]. The mineral form and photovoltaic behavior of Cu_2SnS_3 (CTS) thin films were found firstly by Kovalenker et al. [7] and by Kuku and Fakolujo [8], respectively. Semiconducting copper tin sulfides such as Cu_2SnS_3, Cu_3SnS_4 and $Cu_4Sn_7S_{16}$ could have a significant role in immediate future due to their in-free composition [9]. As a promising absorber material, Cu_2SnS_3 has an absorption coefficient of $10^4\ cm^{-1}$, an electrical conductivity of $10\ \Omega^{-1}\ cm^{-1}$, a hole mobility of $80\ cm^2\ V^{-1}\ s^{-1}$, and a hole concentration of $10^{18}\ cm^{-3}$ [1]. Its optical band gap energy has been reported in between 0.93 and 1.51 eV depending on its crystal structure type [10].

Up to now, CTS thin films have been prepared by various thin film deposition methods such as sulfurizing of electrodeposited Cu–Sn precursors [3], spray pyrolysis technique [9], dc magnetron sputtering [11,12], solid-state reaction [13], and ball milling process [14], sol–gel spin coating [15]. Among them, sol–gel method is a very simple and low-cost process that sulfide films can be directly obtained by sulfurizing oxyhydrate precursors. Furthermore, this method may also provide accurate control of film thickness, particle size and porosity by tuning different parameters such as, precursor concentrations, rotation speed, heat treatment temperature and so on [16].

It is well known that material properties such as surface morphology, crystalline structure, grain size, porosity, brightness, internal stress, pitting, corrosion behavior and even chemical composition can be tuned by using surfactants and used to improve energy conversion efficiency of thin film solar cells to some extent [17]. As a non-ionic surfactant material, Triton-X100® (namely octyl phenol ethoxylate, CAS number: 9002-93-1) exhibits both sterical and electrosterical repulsion when added in the solution [18]. Maldonado-Valdivia et al. [19] reported that the solar cell efficiency may be improved with increasing amount of Triton-X100®. The role of Triton-X100® in CTS deposition process has not been studied yet. Thus, it is of interest to us to investigate the effects of Triton-X100® on morphology, crystallographic structure, electrical properties and photovoltaic response of the Cu_2SnS_3 thin films.

Here we report, for the first time, the results of the Triton-X100® assisted preparation and characterization of CTS thin films obtained by using sol–gel spin coating method and a subsequent annealing in a sulfur atmosphere. The physical characteristics of the films were examined by means of X-ray diffraction, scanning

* Corresponding author. Tel.: +90 3262455845; fax: +90 3262455867.
E-mail address: sinan_yasar@msn.com (S. Yaşar).

http://dx.doi.org/10.1016/j.jallcom.2014.08.196
0925-8388/© 2014 Elsevier B.V. All rights reserved.

electron microscopy, energy dispersive X-ray spectroscopy, photo-transient current and electrical resistivity–temperature measurement.

2. Experimental

CTS thin films were obtained on glass substrates by spinning the solution containing basically copper (II) acetate monohydrate (0.9 M, 98+%), tin (II) chloride (0.5 M, 98%) and thiourea (0.2 M, 99.0+% from Sigma Aldrich) into 2-methoxyethanol (99.8% from Sigma Aldrich). 25 μl of diethanolamine (DEA) were added slowly into the solution as a stabilizer while stirring. According to the literature reports [3,6,20] that copper concentration under stoichiometric value prevents the formation of $Cu_{2-x}S$ or other binary/ternary phases and improve the performance of the film. Therefore, we prepared the starting solution with a Cu/Sn ratio of 1.80. The solution was poured into four beakers and then 0, 1, 2 and 3 at.% of TritonX-100® (from Sigma Aldrich) were added into each solution. The final solutions were stirred at 45 °C, 1000 rpm for 1 h to dissolve all constituents completely. Glass substrates were ultrasonically cleaned in turn with detergent, nitric acid (1:4), acetone and ethanol for 10 min. To produce the CTS films, the prepared solutions were spin-coated onto glass substrates at 3000 rpm for 30 s followed by solvent-drying at 175 °C for 10 min on a hot plate. The spin-coating and solvent-drying processes were repeated 5 times. Finally, the samples were annealed under 1 atm of sulfur atmosphere for 2 h at 550 °C. The heating rate was 5 °C/min. After the annealing process, the samples were allowed to cool naturally to room temperature. The structural, morphological, compositional, optical and electrical properties of the samples were examined by X-ray diffraction (XRD, PANalytical X'Pert PRO MPD with the wavelength of 1.5418 Å Cu Kα radiation at 40 keV accelerating voltage and 35 mA current, step size of 0.05° and scan step time of 1 s), scanning electron microscopy (FEI, Quanta FEG 250), energy dispersive X-ray spectroscopy (EDXS, Oxford Instruments ISIS 300) methods. Photo-transient current of the Ag/n-Si/CTS/Ag structures were obtained at 2 V under different illuminations. The intensity of light was measured with a lux meter (Testo-540). Resistance–temperature characteristics of the samples were investigated by two point probe method in the temperature range of 300–550 K through a Keithley 6487 interfaced with computer by a Labview program.

3. Results and discussions

3.1. Structural results

Fig. 1 shows the obtained XRD patterns of the samples. From Fig. 1, all peaks observed at $2\theta = 15.02°$, 28.37°, 32.00°, 47.31° and 56.22° match with those of reference Cu_2SnS_3 pattern (JCPDS 01-089-4714: Tetragonal, $a = b = 0.5413$ nm, $c = 1.0824$ nm, I-42 m). The peaks correspond to (002), (112), (200), (220) and (312) planes, respectively and they indicate the polycrystalline nature of the films. The highest peak at 28.37° corresponding to (112) plane proves the preferred crystallization. Any peak referring to other binary/ternary phases were not detected in the patterns.

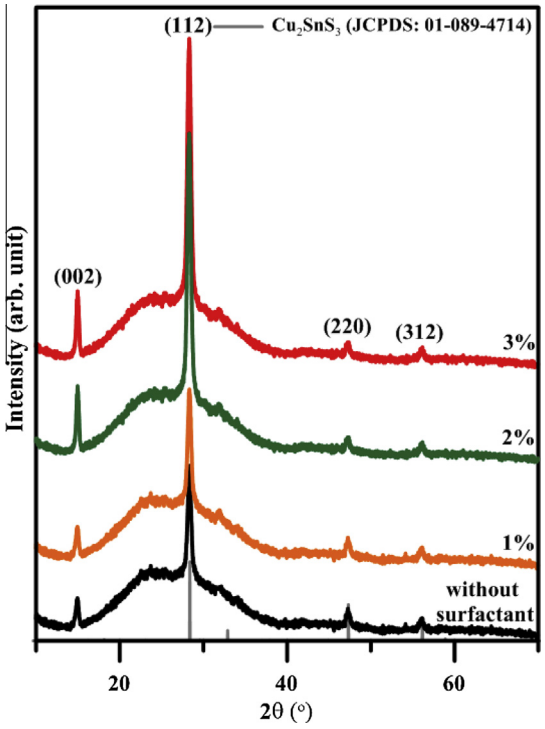

Fig. 1. Obtained X-ray diffraction patterns of the samples prepared with different TritonX-100® amounts.

As can be seen that the intensity of the peaks corresponding to (112) and (002) planes increase with increasing Triton-X100® content. It may be concluded that Triton-X100® enhances the growth of (112) and (002) oriented planes under our experimental conditions.

Through the full width half maximum (FWHM) value of an observed peak in XRD pattern, average crystallite size of a film can be calculated by using the Debye–Scherrer equation [21]:

$$D = 0.94\lambda/\beta\cos\theta \quad (1)$$

where λ is the wavelength of X-ray radiation, θ is the Bragg angle of the peak, and β is the angular width of the peak at full-width at half maximum (*FWHM*). The width of each obtained XRD peak increases because of instrumental and physical factors (crystallite size, strain and dislocation) [22]. The microstrain (ε) and dislocation density (ρ) for preferential orientation were calculated using the formulas given below [23]:

$$\varepsilon = \beta\cos\theta/4 \quad (2)$$

and

$$\rho = 15\varepsilon/aD \quad (3)$$

where a is the lattice constant. The crystallite size estimations of the films were done by taking into account all observed peaks and the estimated values are given in Table 1. According to Table 1, it can be seen that crystallite size of the films increases to some extent with Triton-X100® content. As will be discussed in photo-conversion measurement section, this trend yields an increase in photo-conversion capability of the samples (Section 3.3).

3.2. Morphological and compositional analysis

Fig. 2 shows the SEM images of the CTS films deposited by using 0%, 1%, 2% and 4% (by vol.) of Triton-X100®. From Fig. 2, it can be seen that the surface roughness of the films decreases with increasing Triton-X100® content. The surface of the sample without Triton-X100® (Fig. 2a) has porous and has agglomeration like morphology than those of the samples with Triton-X100® (Fig. 2b–d). It is also clear that, the sample prepared with 3% Triton-X100® (Fig. 2d) is more continuous and without crack than others. As a first conclusion, regarding film morphology, increasing Triton-X100® content in the sol–gel growth solution the smoother and continuous texture can be obtained. This enhancement may decrease the recombination and facilitate transport of photo-induced electrons.

Table 1
Estimated structural results of the samples.

Sample	Without surfactant	1%	2%	3%
Average crystallite size (nm)	17	18	20	23
Microstrain	2.2×10^{-3}	2.1×10^{-3}	1.9×10^{-3}	1.6×10^{-3}
Dislocation density (m^{-2})	2.6×10^{15}	2.4×10^{15}	2.1×10^{15}	1.8×10^{15}

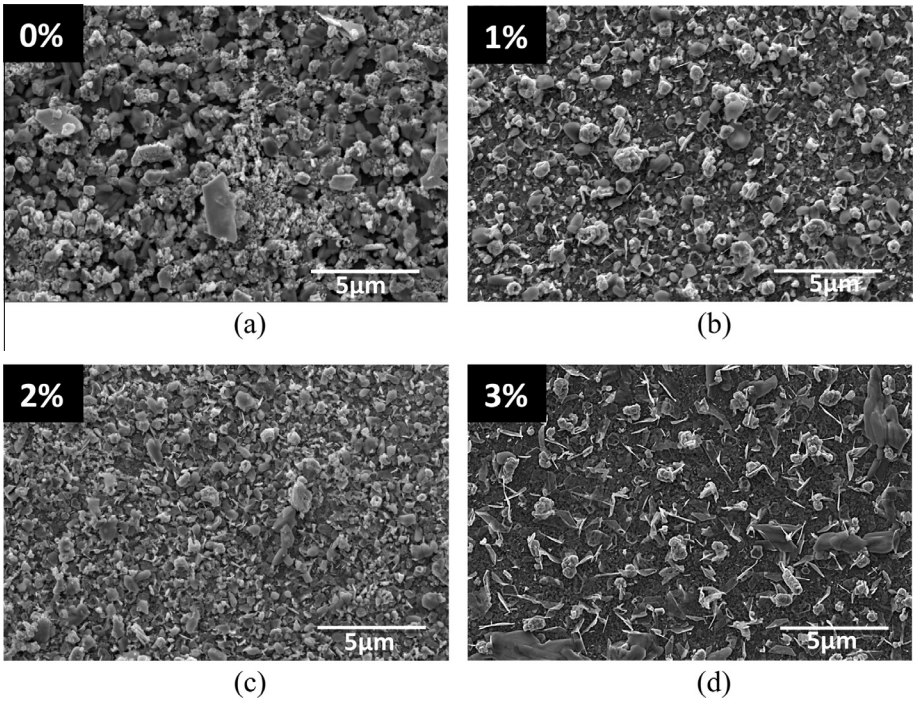

Fig. 2. Plain view SEM images of the samples with (a) 0%, (b) 1%, (c) 2% and (d) 3% TritonX-100®.

Table 2
Energy dispersive X-ray spectroscopy analysis of the films.

Sample	Composition results (at.%)			Cu/Sn	S/metal ion ratio
	Cu	Sn	S		
Without surfactant	27.29	13.92	43.79	1.96	1.06
1%	26.54	13.80	45.75	1.92	1.13
2%	27.73	14.55	44.87	1.91	1.06
3%	28.05	14.18	43.98	1.98	1.04

Maldonado-Valdivia et al. [19] fabricated TiO_2 photo electrodes with Triton-X100® and obtained smooth surface without granular features nor cracks and the lowest number of particle clusters, showing the highest surface homogeneity.

Energy dispersive X-ray spectroscopy analysis of the films (at.%) is given in Table 2. It can be deduced that all obtained films have slightly Cu-poor composition and Triton-X100® content does not change their compositions. The Cu/Sn atomic ratios were found to be 1.96, 1.92, 1.91 and 1.98 for the films growth with 0, 1, 2 and 3 at.%, respectively. Those ratios are almost consistent with the initial ratio of precursor solution (Cu/Sn = 1.80). Additionally, S/metal ratios of the films were found quite close to unity indicating a successful sulfurization process.

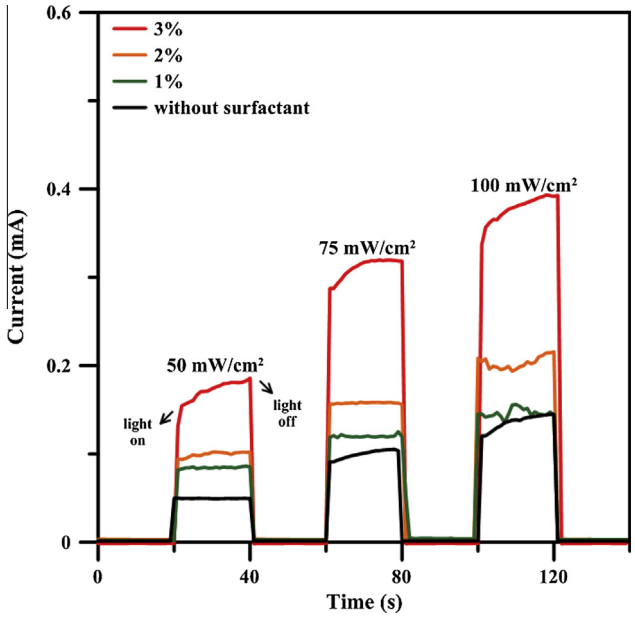

Fig. 3. The photo-transient current curves of the produced Ag/n-Si/CTS/Ag structure at 2.0 V under different illuminations of 50, 75 and 100 W/cm^2.

3.3. Photo-transient current characteristics of the Ag/n-Si/CTS/Ag structure

Ag/n-Si/CTS/Ag hetero-junctions were also fabricated to see the photo-conversion capability of the produced CTS films. The photo-transient current curves of the structures at 2.0 V under different illuminations are shown in Fig. 3. From Fig. 3, it can be seen that the n-Si/CTS junctions exhibit good photo-conductivity and there is a sudden change in the photo-current which confirms photo-sensitivity of the produced structures. The photo-induced current values of the samples increase with increasing Triton-X100® content. This increasing may be resulted from the enhancement occurring on the surface of the samples with increasing Triton-X100®. It has been noted in the previous section; this enhancement may decrease the recombination and facilitate transport of photo-induced electrons. Table 3 shows the light on/light off current ratios (I_{on}/I_{off}) for the n-Si/CTS junctions under

Table 3
Light on/light off current ratios (I_{on}/I_{off}) for the n-Si/CTS junctions under illuminations of 50, 75 and 100 mW cm^{-2}.

Sample	Electrical activation energy (E_A)		Light on/light off current ratio (I_{on}/I_{off}) under different illuminations		
	E_{A1} (meV)	E_{A2} (meV)	50 mW/cm^2	75 mW/cm^2	100 mW/cm^2
Without surfactant	60	250	45	88	126
1%	54	140	78	107	130
2%	91	182	90	142	192
3%	97	200	158	281	347

illuminations of 50, 75 and 100 mW cm^{-2}. From Table 3, it can be seen that maximum I_{on}/I_{off} ratio was achieved for the sample with 3% Triton-X100®.

3.4. Electrical results

Majority carrier type of the films was identified through thermo–emf method [24]. The samples exhibited p-type semiconductor nature thereby the majority carriers were holes. Resistance–temperature characteristics of the samples were examined in the temperature ranges of 300–473 K so that to find impurity levels' electrical activation energies. Theoretical background of the method which we made use of can be summarized as below:

Based on the solid-state theory of semiconductors [25,26], the relation between temperature and dark electrical resistance of a semiconductor film with one or more impurity levels is given by

$$R(T) = R_0 e^{E_g/2kT} + \sum_{i=1}^{n} R'_{0,i} e^{\Delta E_i/kT} \quad (4)$$

In Eq. (4), R_0 and $R'_{0,i}$ are constants, E_g is the thermal band gap energy, ΔE_i is the impurity levels' electrical activation energy, k is Boltzmann's constant, and T is temperature. In a relatively low temperature, the conductivity of a semiconductor film is governed by the charge carriers generated by ionization of impurity levels (extrinsic conductivity), and thus the second term in Eq. (4) controls the R_T value. The temperature dependence of conductivity is governed by the band-to-band transitions at relatively higher temperatures. The charge carriers acquire enough thermal energy to make an inter-band transition (the intrinsic conductivity is "activated" at these temperatures) under certain conditions [25]. According to the discussion above, the each term in Eq. (4) may be used independently in the corresponding temperature intervals. So in the graph of ln(R) vs. 1000/T, a number of linear trends appear

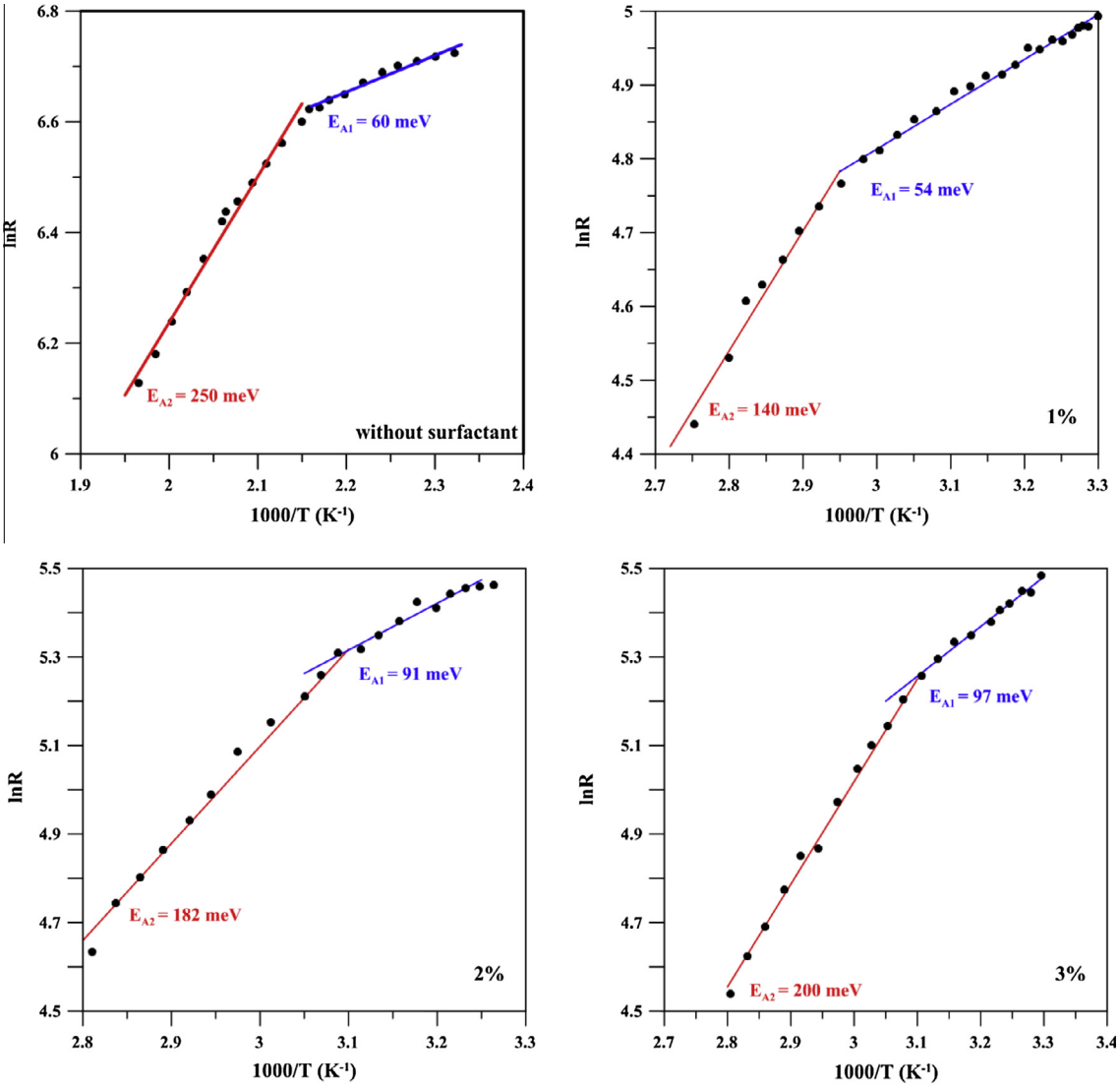

Fig. 4. ln(R) vs. 1000/T graphs of the samples prepared with different TritonX-100® amounts.

which indicate a number of impurity levels. Thus the second term in Eq. (4) determines the R_T dependence in the studied temperature interval (300–473 K). Dark electrical resistance and temperature relation in the region of extrinsic conductivity (corresponding to the lower temperature interval) follows the equation:

$$R(T) = \sum_{i=1}^{n} R'_{0,i} e^{\Delta E_i/kT} \quad (5)$$

Fig. 4 shows ln(R) vs. 1000/T graphs of the samples. The presence of discrete linear regions in Fig. 4 suggests that there are two types of conduction mechanism present in the studied samples. By using Eq. (5), ΔE can be easily written as

$$\Delta E = k \frac{d(\ln R(T))}{d(1/T)} \quad (6)$$

Electrical activation energy values of the impurity levels were estimated from the slopes of ln(R) vs. 1000/T graphs. Two values were estimated for each film and are summarized in Table 3. Impurity level electrical activation energy (ΔE) values of the thin film samples were found in between 54 and 250 meV for samples grown with or without Triton-X100®. There are two studies reporting the electrical activation energies for Cu_2SnS_3 thin films in literature. Bouaziz et al. [10] reported Cu_2SnS_3 thin films synthesized by solid state reaction method and found 25 meV in a temperature interval of 90–300 K. Kahraman et al. [27] reported electrical activation energies for chemically grown Cu_2SnS_3 thin films between 40 and 130 meV in 300–723 K. It can be concluded that the discrete slopes of ln(R) vs. 1000/T graphs prove different conduction mechanism of the films and estimated values are consistent with the literature.

4. Conclusions

In this study, we report the results of the Triton-X100®assisted preparation and characterization of CTS thin films obtained using sol–gel spin coating method and a subsequent annealing in a sulfur atmosphere, for the first time. The physical characteristics of the films were examined by means of X-ray diffraction, scanning electron microscopy, energy dispersive X-ray spectroscopy, photo-transient current and electrical resistivity–temperature measurements. XRD patterns of the samples matched well with the reference Cu_2SnS_3 pattern and indicated the polycrystalline nature of the films. Peaks referring to other binary/ternary phases were not detected in the patterns.

With increasing Triton-X100® content, crystallite size of the films increased whereas surface roughness of the films decreased. Triton-X100® content in the sol–gel growth solution resulted smoother and continuous texture.

Photo-conductivity behaviors of the n-Si/CTS junctions confirmed the photo-sensitivity of the structures. The photo-induced current values of the samples increased with increasing Triton-X100®content. That increasing in the photo-current was attributed to transport of photo-induced electrons facilitated with decreasing recombination resulted from the surface enhancement of the films. The presence of discrete linear regions in the resistance–temperature plots of the films suggested two types of electrical conduction mechanism. Finally, growth of Cu_2SnS_3 thin films with Triton-X100®surfactant may be a convenient and efficient way to improve conversion efficiency of Cu_2SnS_3 based solar cell applications.

Acknowledgement

The financial support from Scientific Research Commission of Mustafa Kemal University (Project No: 11680) is greatly appreciated.

References

[1] M. Ristov, G. Sinadinovski, M. Mitreski, M. Ristova, Photovoltaic cells based on chemically deposited p-type SnS, Sol. Energy Mater. Sol. Cells 69 (2001) 17–24.
[2] Z. Su, K. Sun, Z. Han, F. Liu, Y. Lai, J. Li, Y. Liu, Fabrication of ternary Cu–Sn–S sulfides by a modified successive ionic layer adsorption and reaction (SILAR) method, J. Mater. Chem. 22 (2012) 16346–16352.
[3] J. Koike, K. Chino, N. Aihara, H. Araki, R. Nakamura, K. Jimbo, H. Katagiri, Cu_2SnS_3 Thin-Film Solar Cells from Electroplated Precursors, Jpn. J. Appl. Phys. 51 (2012). 10NC34-10NC34-3.
[4] D. Avellaneda, M.T.S. Nair, P.K. Nai, Cu_2SnS_3 and Cu_4SnS_4 Thin films via chemical deposition for photovoltaic application, J. Electrochem. Soc. 157 (2010) D346–D352.
[5] D. Tiwari, T.K. Chaudhuri, T. Shripathi, U. Deshpande, Cu_2SnS_3 as a potential absorber for thin film solar cells, AIP Conf. Proc. 1447 (2012) 1039.
[6] K. Chino, J. Koike, S. Eguchi, H. Araki, R. Nakamura, K. Jimbo, H. Katagiri, Preparation of Cu_2SnS_3 thin films by sulfurization of Cu/Sn stacked precursors, Jpn. J. Appl. Phys. 51 (2012). 10NC35-10NC35-4.
[7] V.A. Kovalenker, V.S. Malov, T.L. Yevstigneyeva, L.N. Vyalsov, Mohite, Cu_2SnS_3, a new sulfide of tin and copper, Int. Geol. Rev. 25 (1983) 117–120.
[8] T.A. Kuku, O.A. Fakolujo, Photovoltaic characteristics of thin films of Cu_2SnS_3, Sol. Energy Mater. 16 (1987) 199–204.
[9] M. Bouaziz, M. Amlouk, S. Belgacem, Structural and optical properties of Cu_2SnS_3 sprayed thin films, Thin Solid Films 517 (2009) 2527–2530.
[10] M. Bouaziz, J. Ouerfelli, S. Srivastava, J. Bernde, M. Amlouk, Growth of Cu_2SnS_3 thin films by solid reaction under sulphur atmosphere, Vacuum 85 (2011) 783–786.
[11] P. Fernandes, P. Salome, A. Cunha, A study of ternary Cu_2SnS_3 and Cu_3SnS_4 thin films prepared by sulfurizing stacked metal precursors, J. Phys. D: Appl. Phys. 43 (2010) 215403–215413.
[12] P.A. Fernandes, P.M.P. Salome, A.F. Cunha, Study of polycrystalline Cu_2ZnSnS_4 films by Raman scattering, J. Alloys Comp. 509 (2011) 7600–7606.
[13] M. Onoda, X.-A. Chen, A. Sato, H. Wada, Crystal structure and twinning of monoclinic Cu_2SnS_3, Mater. Res. Bull. 35 (2000) 1563.
[14] Q. Chen, X. Dou, Y. Ni, S. Cheng, S. Zhuang, Study and enhance the photovoltaic properties of narrow-bandgap Cu_2SnS_3 solar cell by p–n junction interface modification, J. Colloid Interface Sci. 376 (2012) 327–330.
[15] H. Dahman, S. Rabaoui, A. Alyamani, L. El Mir, Structural, morphological and optical properties of Cu_2SnS_3 thin film synthesized by spin coating technique, Vacuum 101 (2014) 208–211.
[16] Md. M. Rahman, H. Tanaka, T. Soga, T. Jimbo, and M. Umenot, Effect of sol processing parameters on dye-sensitized TiO2 solar cell by spin-coating method, Photovoltaic Specialists Conference, 2000. Conference Record of the Twenty-Eighth IEEE, 806–809.
[17] M. Mouanga, L. Ricq, G. Douglade, J. Douglade, P. Berçot, Influence of coumarin on zinc electrodeposition, Surf. Coat. Technol. 201 (2006) 762–767.
[18] S. Xu, C. Zhou, Y. Yang, H. Hu, B. Sebo, B. Chen, Q. Tai, X. Zhao, Effects of ethanol on optimizing porous films of dye-sensitized solar cells, Energy Fuels 25–3 (2011) 1168–1172.
[19] A.I. Maldonado-Valdivia, E.G. Galindo, M.J. Ariza, M.J. García-Salinas, Surfactant influence in the performance of titanium dioxide photoelectrodes for dye-sensitized solar cells, Sol. Energy 91 (2013) 263–272.
[20] S. Chen, X.G. Gong, A. Walsh, S. Wei, Defect physics of the kesterite thin-film solar cell absorber Cu_2ZnSnS_4, Appl. Phys. Lett. 96 (2010). 021902-021902-3.
[21] V. Pecharsky, P. Zavalij, Fundamentals of Powder Diffraction and Structural Characterization of Materials, Springer, New York, 2005.
[22] H.P. Klug, L. Alexander, X-ray Diffraction Procedures for Polycrystalline and Amorphous Materials, John Wiley & Sons, New York, 1974.
[23] A. Suresh, K. Chatterjee, V.K. Sharma, S. Ganguly, K. Kargupta, D. Banerjee, Effect of pH on structural and electrical properties of electrodeposited Bi_2Te_3 thin films, J. Elect. Mater. 38 (2009) 449–452.
[24] K. Seeger, Semiconductor Physics, Springer, Berlin/Wien/New York, 1973.
[25] B. Pejova, A. Tanusevski, I. Grozdanov, Photophysics, photoelectrical properties and photoconductivity relaxation dynamics of quantum-sized bismuth(III) sulfide thin films, J. Solid State Chem. 178 (2005) 1786–1798.
[26] S. Kahraman, M. Podlogar, S. Bernik, H.S. Güder, Facile synthesis of Cu_2ZnSnS_4 photovoltaic absorber thin films via sulfurization of Cu_2SnS_3/ZnS layers, Metall. Mater. Trans. A 45 (2014) 2326–2334.
[27] S. Kahraman, S. Çetinkaya, H.M. Çakmak, H.A. Çetinkara, H.S. Güder, Cu_2SnS_3 absorber thin films prepared by successive ionic layer adsorption and reaction method, Int. J. Mater. Res. 104 (2013) 1020–1027.